

# THE CENTRIOLE CYCLE IN SYNCHRONIZED HELA CELLS

ELLIOTT ROBBINS, GISELA JENTZSCH,  
and ANITA MICALI

From the Departments of Cell Biology, Microbiology, and Immunology, the Albert Einstein College of Medicine, Bronx, New York 10461

## ABSTRACT

Progression of the HeLa cell through its life cycle is accompanied by centriolar replication and pericentriolar changes that are in synchrony with DNA synthesis and mitosis. The first signs of preparation for replication occur during  $G_1$  at which time the two orthogonal centrioles separate. Replication by budding begins at/or near the initiation of DNA synthesis and is completed by  $G_2$ . Pericentriolar changes which probably are causally related to spindle tubule formation occur at this time and include the appearance of vesicles, electron-opaque bodies, and an amorphous pericentriolar halo. These phenomena begin to disappear by late prophase, and the remainder of mitosis manifests decreasing centriolar and pericentriolar activity.

Centriole replication by orthogonal budding from a parent centriole has been described in both the light and electron microscopes (1-3). Its temporal relationship to the telophase stage of the cell cycle has been inferred, in sea urchin, from the morphological modification of cell division induced by mercaptoethanol (4), and Cleveland's extensive work on centriole replication in flagellates is well known (5). In mammalian cells, replication is assumed to occur sometime during interphase; however, the lack of more precise data is due in large part to the dearth of morphological criteria which might distinguish individual segments of interphase. In the present study, the use of synchronized cells (6) has made it possible to examine centriolar morphology in the  $G_1$ , S,  $G_2$ , or mitotic phases of the cell division cycle and, in certain cases, specific cells have been selected for electron microscopy after light microscope examination (7). We have found that the two centrioles present in  $G_1$  commence replication at about the same time that DNA synthesis begins, and that the process is

completed by the end of S.<sup>1</sup> Recognizable centriolar and pericentriolar transitions occur during S,  $G_2$ , and prophase, while metaphase, anaphase, telophase, and  $G_1$  are stages of regressive change or relative inactivity.

## MATERIAL AND METHODS

HeLa cells of the  $S_3$  strain were used throughout. Methods for obtaining populations of synchronized cells and for following them through interphase by monitoring thymidine-<sup>14</sup>C incorporation have been described in detail (6), as has the technique of selecting individual cells for electron microscopy (7). With these two techniques, cells at various points in the life cycle were selected, then fixed, and prepared for microscopy by a rapid embedding schedule which takes advantage of the partial solubility of Epon 812 in water (8). Ribbons of serial sections were cut on the LKB Ultratome III with a diamond knife and

<sup>1</sup>Although precise timing of the life cycle for an individual cell is not possible even in a synchronized population, the reference to a late  $G_1$  cell or any early S cell is considered a fairly close approximation.

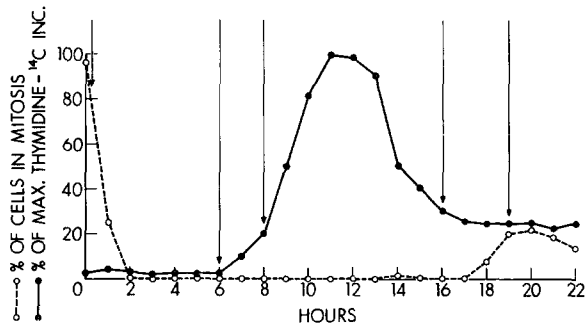
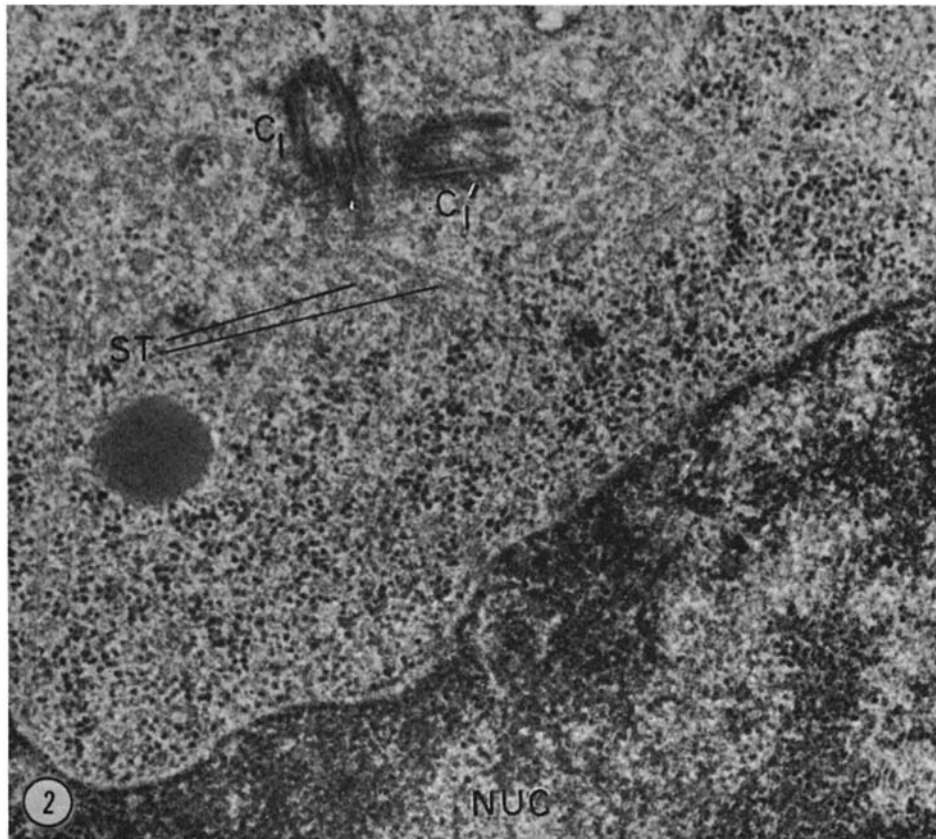


FIGURE 1 Curves show thymidine-<sup>14</sup>C incorporation into DNA of synchronized HeLa cells during life cycle. Mitotic index is plotted on same coordinates. Arrows indicate points in cycle at which aliquots of cells were fixed for electron microscopy. Although almost all cells were in mitosis at the start, they are only partially synchronous by the end of one cycle, as emphasized by broad mitotic index (cells in mitosis/total cells) peak between 17 and 22 hr.



*Abbreviations*

- |   |                                  |
|---|----------------------------------|
| <i>C</i> <sub>1</sub> , centriole 1             | <i>NUC</i> , nucleus             |
| <i>C</i> <sub>1</sub> ' , replicate centriole 1 | <i>PCH</i> , pericentriolar halo |
| <i>C</i> <sub>2</sub> , centriole 2             | <i>ST</i> , spindle tubule       |
| <i>C</i> <sub>2</sub> ' , replicate centriole 2 | <i>VES</i> , vesicles            |
| <i>DB</i> , dense bodies                        |                                  |

FIGURE 2 Telophase cell showing two closely juxtaposed, equal-sized centrioles at right angles to each other. Remnants of mitotic spindle are still visible in centrosomal area. Note relative paucity of ribosomes in immediate vicinity.  $\times 42,000$ .

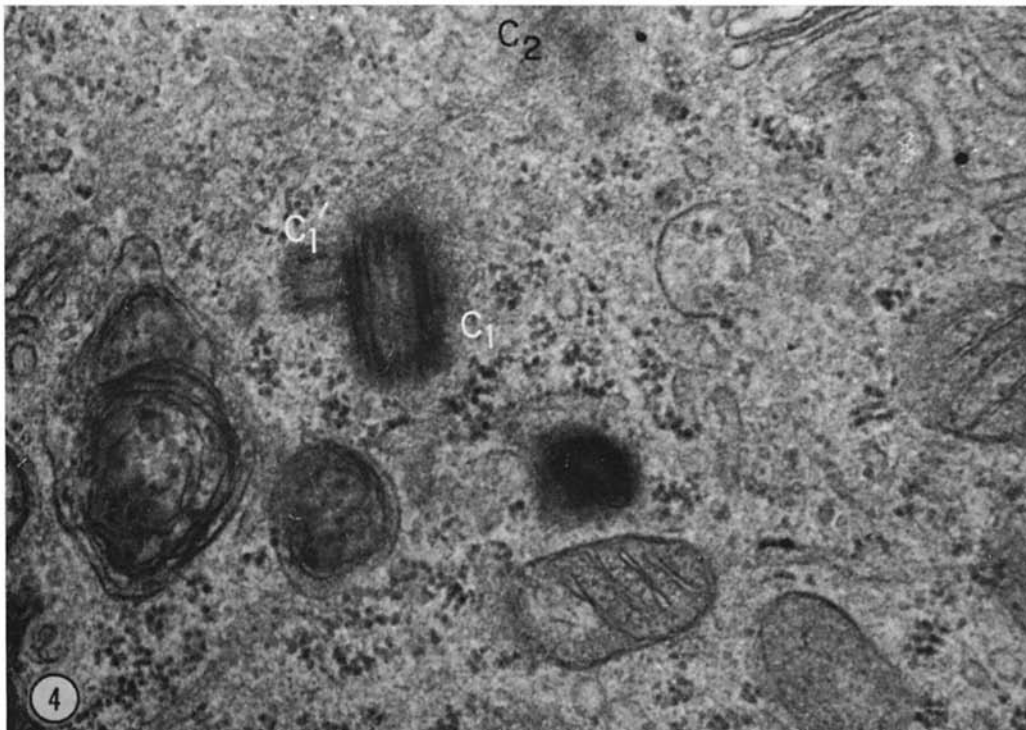
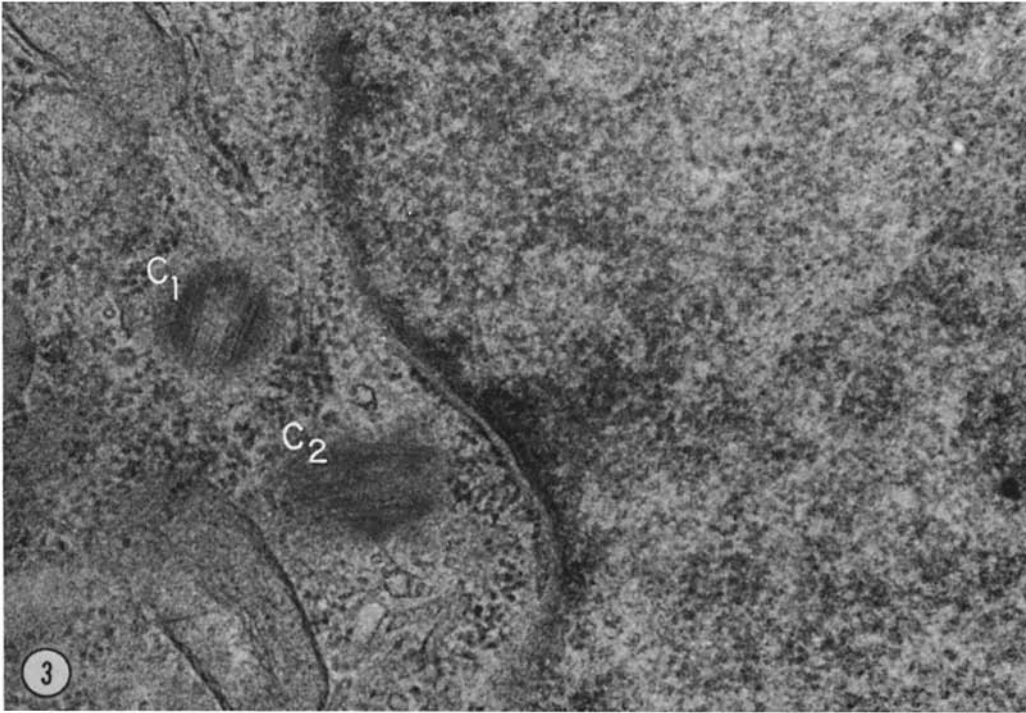


FIGURE 3 Late  $G_1$  centrioles. Note separation of centrioles, absence of orthogonal arrangement, and undefined centrosome.  $\times 52,000$ .

FIGURE 4 Early S centriolar complex. Procentriole is seen budding from parent centriole. Second centriolar pair is just coming into plane of section ( $C_2$ ).  $\times 52,000$ .

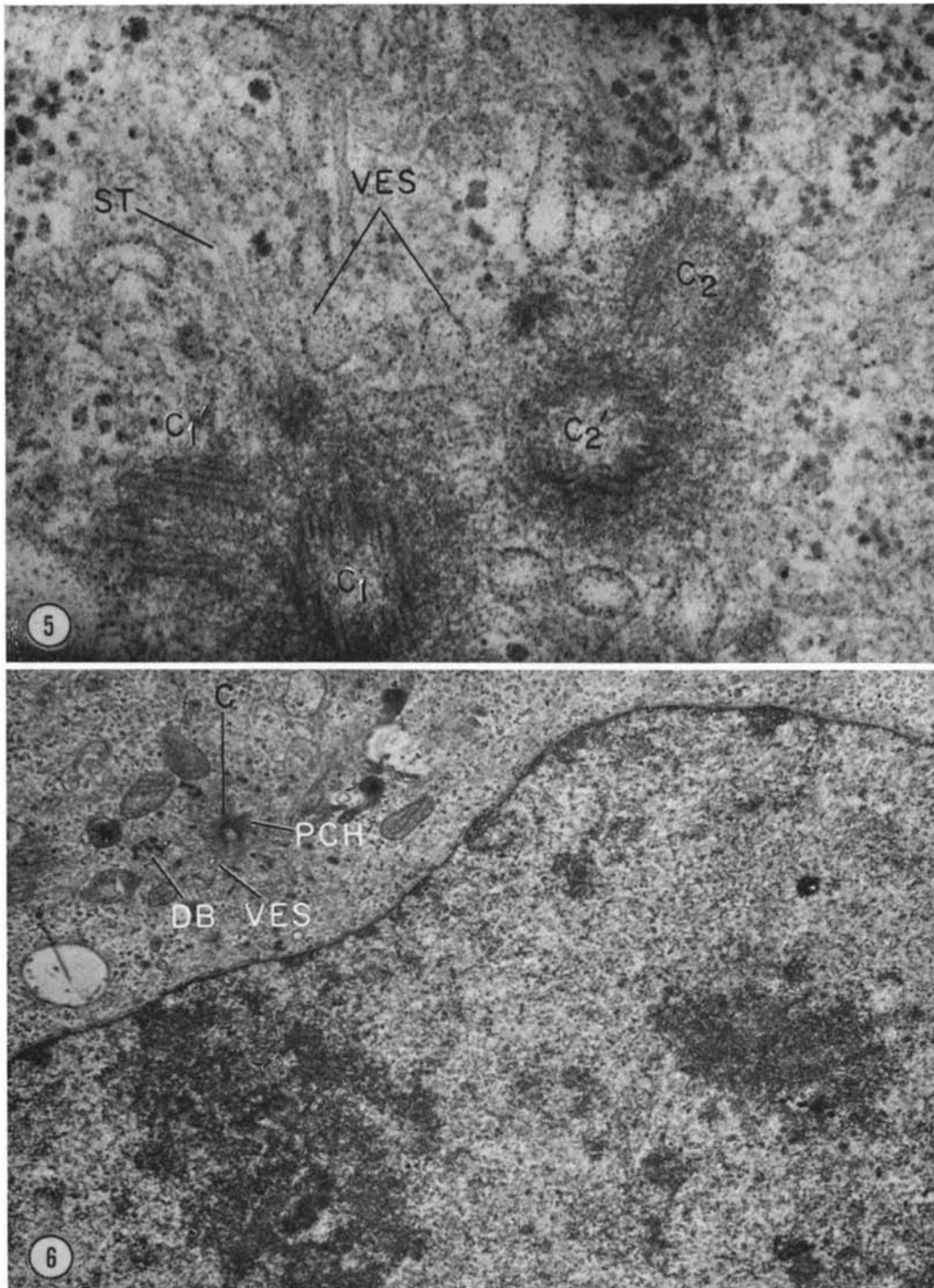


FIGURE 5 Centriolar complex of late S cell showing four full-sized centrioles as two orthogonal pairs. Note occasional spindle tubules and increased number of closely associated membrane-bounded vesicles.  $\times 83,000$ .

FIGURE 6 Very early prophase cell with centriolar complex characteristic of  $G_2$  and the first few minutes of prophase. Note radially dispersed, amorphous osmiophilic bodies which are scattered among neighboring cytoplasmic organelles. C, centriole.  $\times 12,500$ .

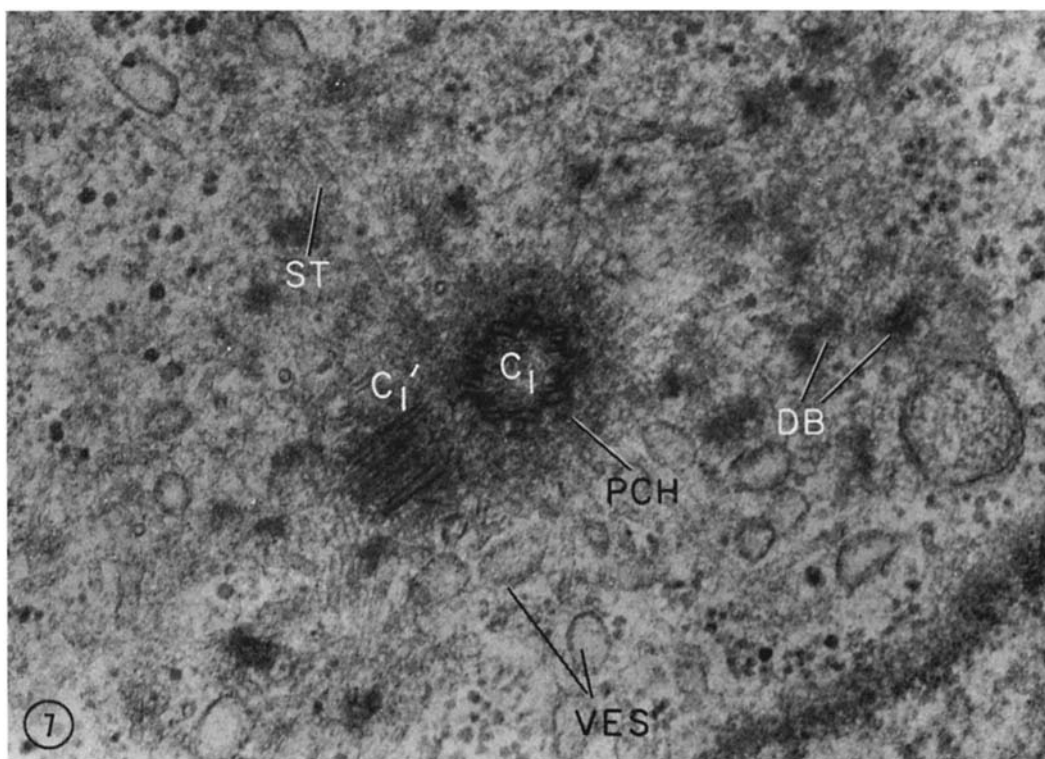


FIGURE 7 Higher magnification of centriolar complex from subsequent section of cell in Fig. 6. Centriole pair is seen amidst numerous, amorphous electron-opaque bodies. The bodies possess no limiting membrane and extend for a radius of about 700 Å from the centriolar center. There is a relatively well-circumscribed, electron-opaque halo surrounding one of the centrioles. Radially distributed membrane-bounded vesicles and incipient spindle tubules are also seen. Ribosomes are largely excluded from the centrosome.  $\times 56,500$ .

mounted on LKB single slit grids previously coated with 0.3% Formvar. Only grids on which sections were established to be precisely consecutive were used. Each cell was then followed through several dozen sections, and the morphology as well as the number of centrioles were recorded photographically during the  $G_1$ , S,  $G_2$ , and mitotic phases. Microscopy was done with the Siemens Elmskop IIA with a 50  $\mu$  aperture and 80 kv accelerating voltage.

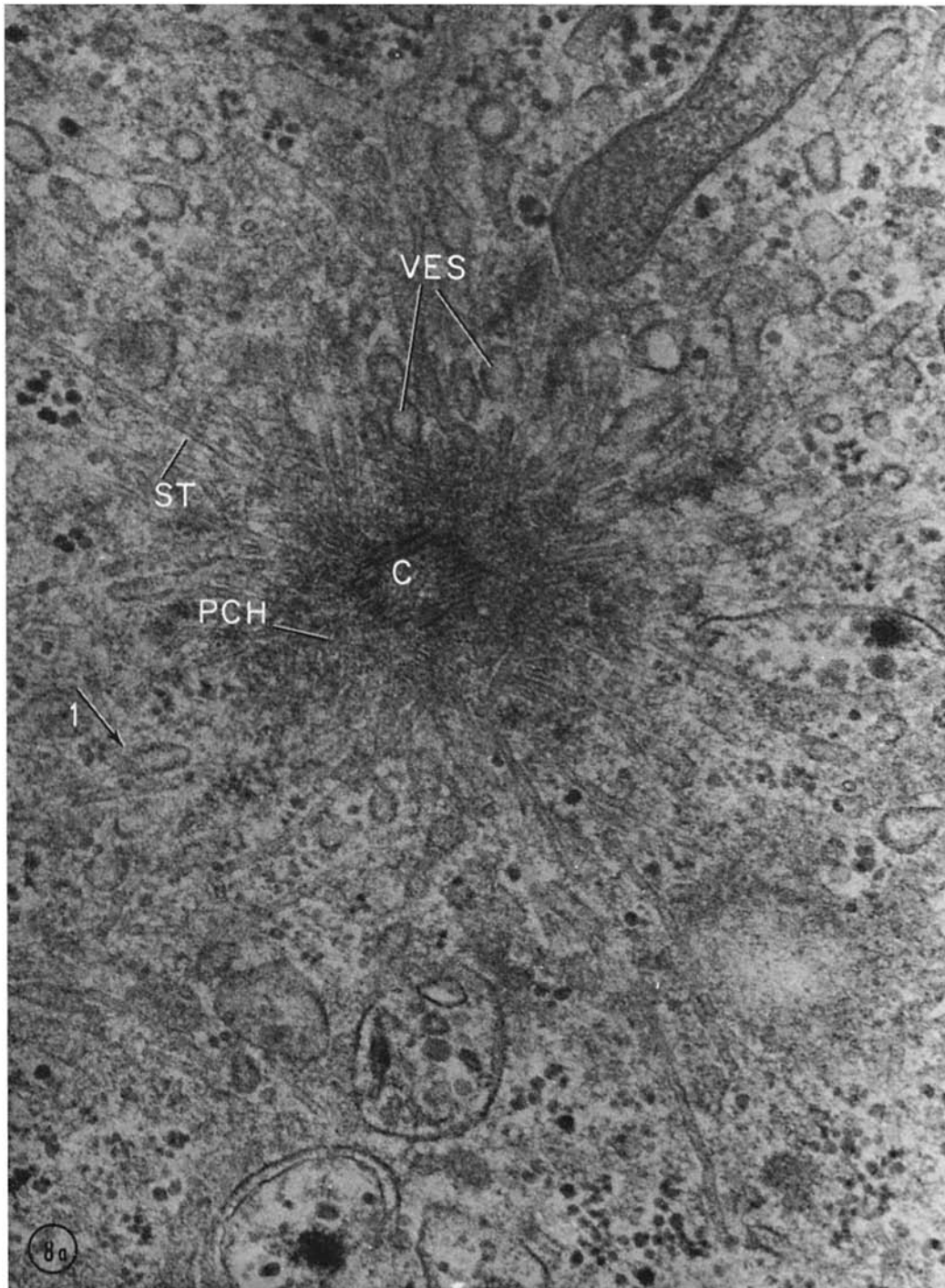
#### RESULTS AND DISCUSSION

Fig. 1 shows a composite curve for mitotic index and thymidine- $^{14}\text{C}$  incorporation in synchronized cells prepared by selective detachment of mitotic cells from monolayer cultures. DNA synthesis follows the well-known curve which is the basis for dividing the cycle into  $G_1$  (presynthesis), S (DNA synthesis)  $G_2$  (postsynthesis), and mitosis, as indicated. Arrows indicate points in the life cycle

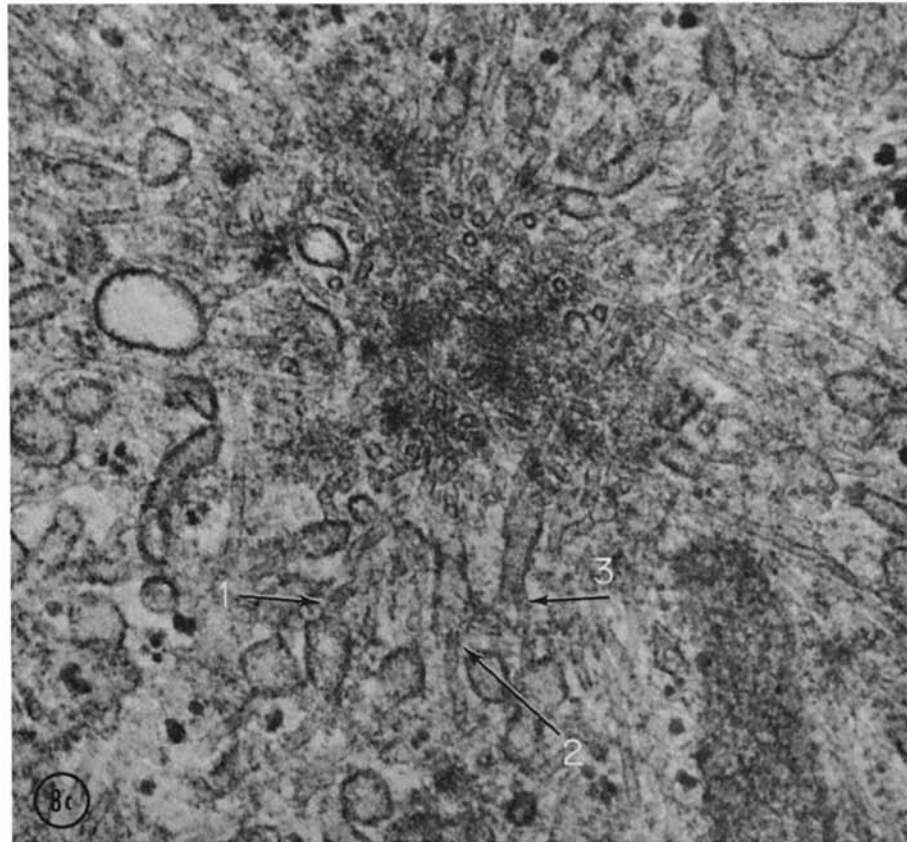
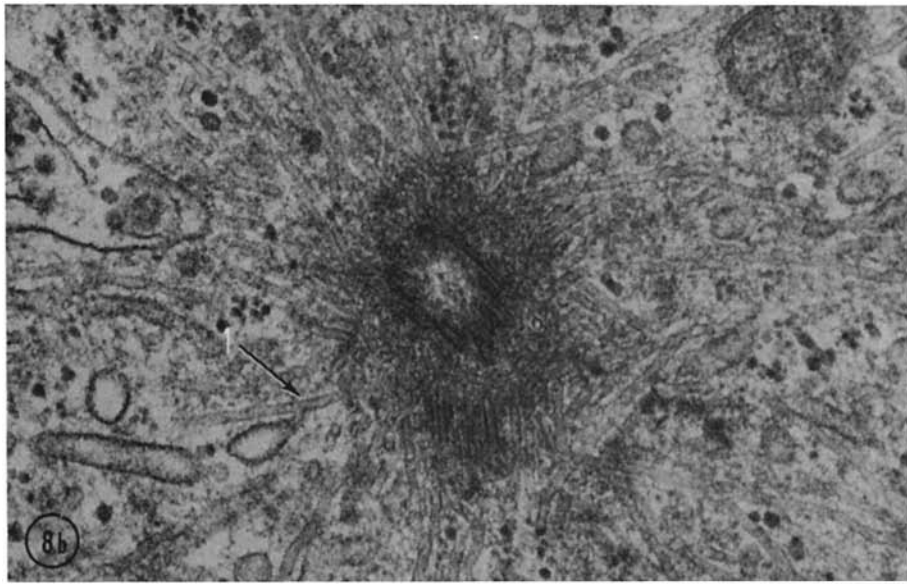
at which aliquots of the synchronized cell suspension were fixed for electron microscopy.

At telophase, immediately prior to entry into  $G_1$ , each daughter cell contains closely associated centrioles in orthogonal array (Fig. 2). In this figure they are approximately equal in size, and the dimensional length is the maximum that we have derived from serial sections; thus the equality in size does not appear to be an artifact of sectioning. The centriolar complex is relatively devoid of ribosomes or other cellular organelles. Remnant spindle tubules showing a radial orientation are still evident, but the association is focal; and the tubules no longer extend to the expanding chromosomes or even to the newly reformed nuclear membrane.

By the end of  $G_1$  it is difficult to find two centrioles in the close juxtaposition seen in Fig. 2, and



FIGURES 8 *a-c* Three serial sections through mid-prophase centriole (*C*). Amorphous electron-opaque bodies have disappeared, but vesicles remain. Pericentriolar halo has expanded to a radius of about  $1 \mu$ . Numbered arrows indicate examples of physical continuity between pericentriolar vesicles and newly forming spindle tubules. Spindle tubules can be followed for several microns in all directions. Figs. 8 *a-b*,  $\times 58,000$ ; Fig. 8 *c*,  $\times 76,500$ .



FIGURES 8 *b* and *c* See legend under Fig. 8 *a*.

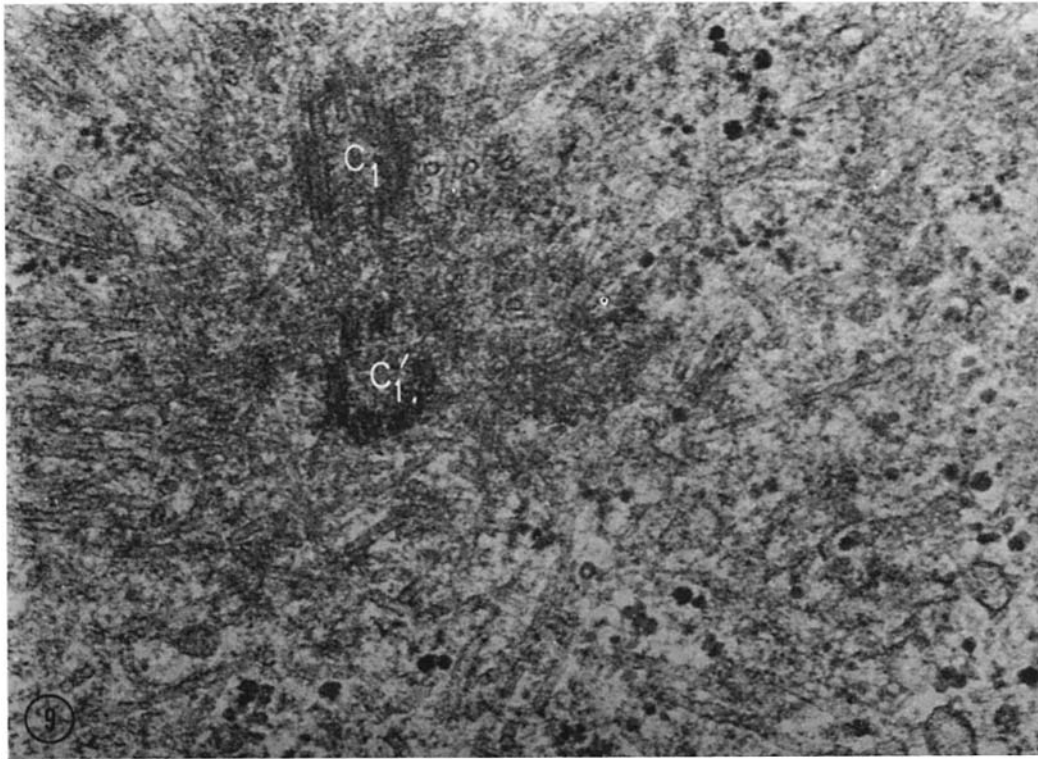


FIGURE 9 Early metaphase centriolar complex. Note partial disappearance of peripheral electron-opaque halo and membrane-bounded vesicles, although spindle tubules remain prominent.  $\times 57,000$ .

most cells examined (80%) showed patterns such as that seen in Fig. 3. The distance between the two centrioles is significantly increased, and the orthogonal arrangement of telophase was very rarely observed even in three-dimensional reconstruction. Only an occasional spindle tubule is visible in the centrosome. Ribosomes are frequently in close apposition, and a clearly defined centrosome is not present. The absence of the centrosome, a structure whose character most likely reflects centriole activity, suggests that, aside from the separatory movement,  $G_1$  is a phase of centriolar quiescence. This discrepancy between our findings and those of Mazia et al. (4) are, in all probability, due to the short generation time of their marine eggs compared to the 17 hr life cycle of the HeLa cell.

2 hr after the incorporation of thymidine- $^{14}C$  is first detectable in pulse-labeled cells, and 2 hr beyond the stage shown in Fig. 3, early stages of centriole replication are seen in about 65–70% of the population. Fig. 4 shows the classical picture

of orthogonal procentriole formation (1–3) with an immature bud protruding asymmetrically from the parent. This section has barely grazed part of the second pair of centrioles ( $C_2$ ) which appeared in similar array in a subsequent field. The absence of the replicating configuration in about 30% of the cells examined at this time in the cycle is attributable to the lack of perfect cell synchrony, since radioautographs confirm that this fraction of the population also fails to incorporate thymidine- $^3H$ . By late S when 100% of the cells are labeled, all cells show centriole replication.

This process of centriole replication appears to occupy most or all of S, since it is only in samples fixed at the end of this stage that we ever see four centrioles whose dimensions approach the maximum for this organelle (Fig. 5). This illustration was used despite the presence of finely scattered lead precipitate overlying the complex, because of the extreme rarity with which all four completed centrioles are seen in a single section. There is an increase in associated membrane-bounded vesicles,



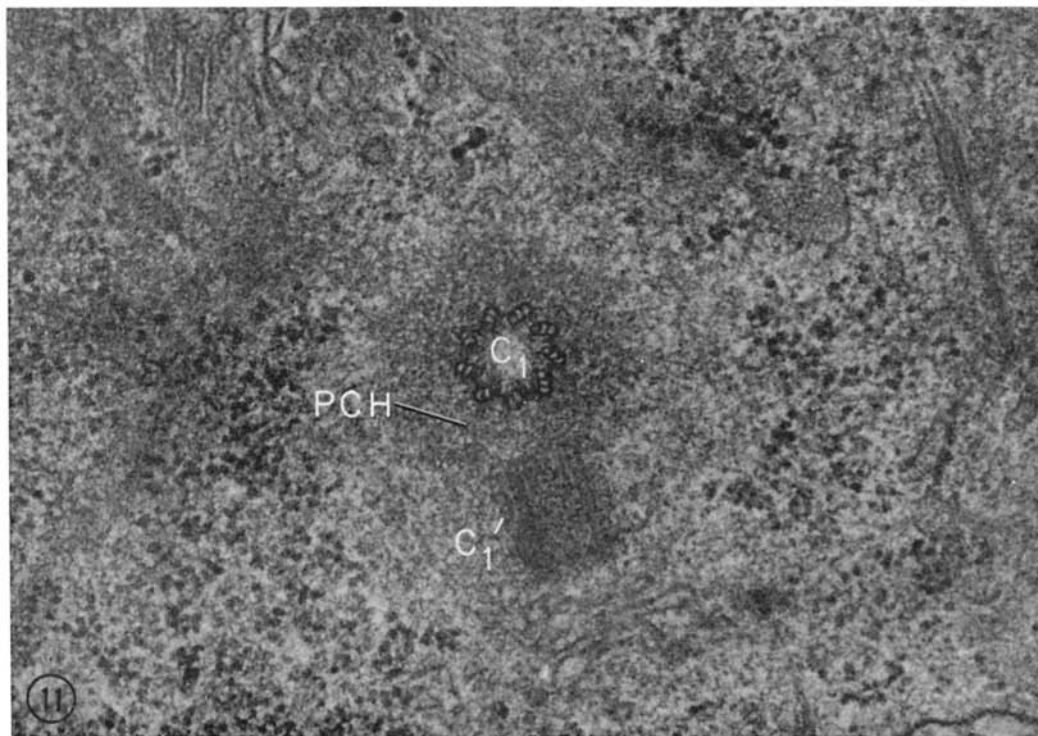
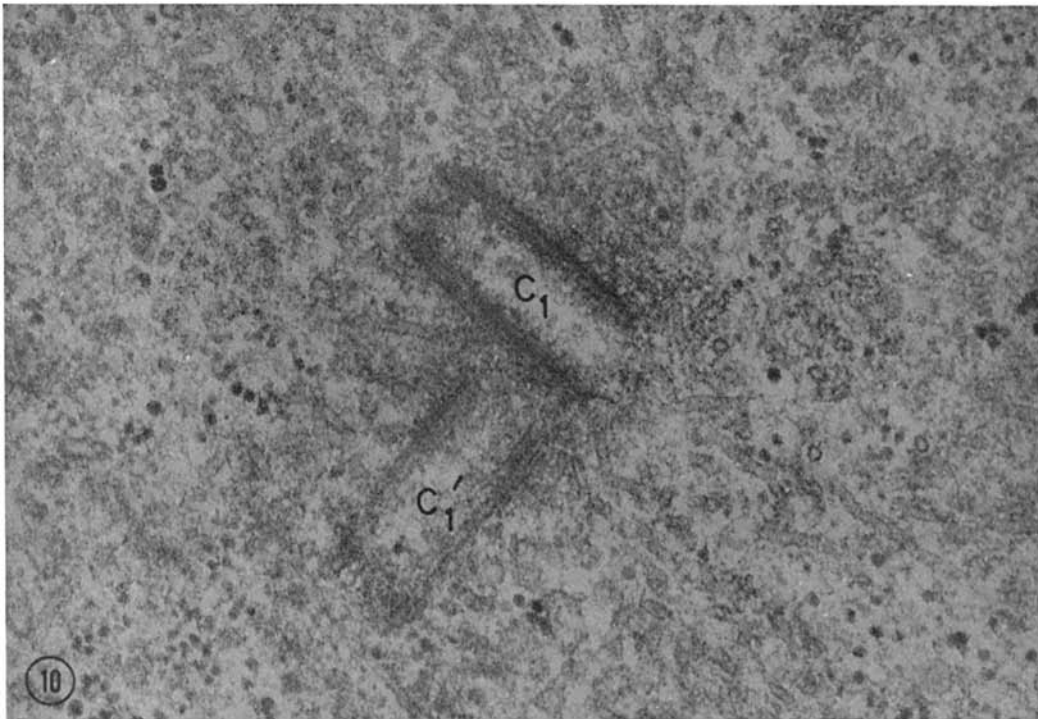


FIGURE 10 Late metaphase centriolar complex. Peripheral electron-opaque halo is completely gone. Orthogonal arrangement of the two equal-sized centrioles is evident.  $\times 63,500$ .

FIGURE 11 Mid-prophase cell treated 3 hr previously with 0.1  $\gamma$ /ml of colchicine. Pericentriolar halo is present although less intensely osmiophilic than in comparable, untreated prophase cell. Note hyaline centrosome, absence of spindle tubules and paucity of membrane-bounded vesicles.  $\times 62,500$ .

and occasional, randomly radiating spindle tubules are seen. Two electron-opaque bodies about 400 Å in diameter are in close relationship with the centriole proper; these are early examples of a more extensive accumulation which takes place in G<sub>2</sub> and lasts until early prophase. The nuclear membrane and nucleoli are still intact in Fig. 6, but the earliest beginnings of chromosome condensation indicate that the cell has just passed the transition between G<sub>2</sub> and prophase. The dispersion of electron-opaque bodies over a wide radius of about 2 μ is now apparent, as is a single centriole in their midst. Although these bodies are similar to pericentriolar satellites (2), they have a wider radius of distribution and are considerably more numerous. Subsequent sections established that at this stage migration of the centriole pairs had already taken place. Fig. 7 shows details of this phase in another section. There is increased formation of both pericentriolar vesicles and spindle tubules. In addition, a peripheral "halo" accumulation of electron-opaque material, probably representing Kawamura's SH-containing material, is noted around one of the two centrioles. This predilection for one centriole may reflect that it alone participates in spindle tubule formation. It should be mentioned here that the halo is not a result of microtubule concentration at this level since it disappears during metaphase at which time microtubules are still present; it also forms in the presence of colchicine which inhibits microtubule generation (see below).

During the succeeding 5 min of prophase, the halo expands rapidly. Cells fixed and individually selected at this time display the centriolar complex shown in Fig. 8. The radially distributed electron-opaque bodies of G<sub>2</sub> or early prophase have all disappeared, and the intense osmiophilic halo (9), along with the extensive, radially disposed spindle tubules, now predominate. The vesicles noted earlier still remain. This close temporal relationship between the electron-opaque bodies of G<sub>2</sub> and early prophase, the pericentriolar halo of later prophase, and the appearance of spindle tubules strongly suggests a causal relation. In support of this hypothesis, we note that, besides showing the temporal relationship, Figs. 8 *a-c* contain numerous examples of actual physical continuity between pericentriolar vesicles and the nascent spindle tubules. These continuities are indicated by

numbered arrows. In Fig. 8 *b*, arrow 1 depicts a bifurcation in a spindle tubule which then ends blindly in a vesicle. Although these examples could arise as a result of structures superimposed within the thickness of the section, it is unlikely since prophase is the only time that such interrelationships between spindle tubules and vesicles are found. In addition, the contours of one often follow the contours of the other. It is also noteworthy that the osmiophilic halo begins to disappear early in metaphase (Fig. 9) at which time spindle formation is complete, and that by the end of metaphase it is absent (Fig. 10); again this suggests some causal relationship. The centriolar complex then bears a close resemblance to that already shown for the telophase cell in Fig. 2, and thereby completes the cycle. The anaphase centriole is not pictured since it is essentially the same in telophase and has been illustrated in an earlier publication (9).

Although the pericentriolar halo exhibits a cyclic pattern consistent with its hypothetical role in spindle tubule elaboration, this cyclic pattern occurs when spindle tubule formation is inhibited by colchicine. Fig. 11 shows a distinct, albeit less pronounced osmiophilic halo surrounding one centriole of a colchicine-treated cell in mid-prophase. No spindle tubules are visible and, in contrast to the normal cell, only an occasional vesicle is seen in the centriolar vicinity, which is consistent with the suggestion that the vesicles are possible precursors of the tubules themselves. As in the untreated cell of Fig. 10, by the end of metaphase the peripheral halo has disappeared.

These data suggest that metaphase, anaphase, and telophase, although they are the periods classically used for centriolar demonstration, are in fact periods of declining centriolar activity, while S, G<sub>2</sub>, and prophase are the phases of striking transitions.

This work was supported by grants GM 14582, AI-4153, and by grants from the National Science Foundation and American Cancer Society. Dr. E. Robbins was a recipient of the Research Career Development Award from the National Institute of General Medical Science.

We are grateful to Mr. David Abramson for astute observations and discussion.

*Received for publication 9 August 1967, and in revised form 3 October 1967.*

#### REFERENCES

1. BERNHARD, W., and E. DE HARVEN. 1960. Fourth International Conference on Electron Microscopy, Berlin, 10-17 September 1958. W. Bargmann, D. Petirs, and C. Wolpers, editors. Springer Verlag, Berlin. 2:217.
2. GALL, J. 1961. *J. Biophys. Biochem. Cytol.* **10**:163.
3. SCHREINER, A., and K. SCHREINER. 1905. *Arch. Biol.* **21**:315. (Cited by J. Gall. 1961. *J. Biophys. Biochem. Cytol.* **10**:163.)
4. MAZIA, D., P. HARRIS, and T. BIBRING. 1960. *J. Biophys. Biochem. Cytol.* **7**:1.
5. CLEVELAND, L. R. 1957. *J. Protozool.* **4**:230.
6. ROBBINS, E., and M. D. SCHARFF. 1966. Cell Synchrony-Studies in Biosynthetic Regulation. I. Cameron and G. Padilla, editors. Academic Press Inc., New York. 353.
7. ROBBINS, E., and N. K. GONATOS. 1964. *J. Cell Biol.* **20**:356.
8. ROBBINS, E., and G. JENTZSCH. 1967. *J. Histochem. Cytochem.* **15**:181.
9. ROBBINS, E., and N. K. GONATOS. 1964. *J. Cell Biol.* **21**:429.